University of Bath

Development of novel building composites based on hemp and multi-functional silica matrix

Atif Hussain[a, b,*], Juliana Calabria-Holley[a], Mike Lawrence[a], Martin P. Ansell[a], Yunhong Jiang[a], Diane Schorr[b], Pierre Blanchet[b]

[a]BRE Centre for Innovative Construction Materials, Department of Architecture and Civil Engineering, University of Bath, Bath BA2 7AY, UK

[b]Department of Wood and Forest Sciences, Université Laval, Quebec, QC, G1V 0A6, Canada

*Corresponding Author: Atif Hussain (A.Hussain@bath.ac.uk)

Abstract

This study focuses on the development of novel bio-composites using a silica matrix that provides dual functionality: as a hydrophobic surface treatment and as a binder for hemp-shiv. The hydrophilic nature of hemp shiv, a plant based aggregate, results in composites having poor interfacial adhesion, weak mechanical properties and long drying times. In this work, sol-gel process has been utilised to manufacture durable low density hemp based composites. Morphological characterisation by scanning electron microscopy (SEM) showed that hemp shiv was embedded well in the matrix. Detailed chemical analysis using x-ray photoelectron spectroscopy (XPS) and gas chromatography-mass spectrometry (GC-MS) indicate the presence of water soluble and ethanol soluble extractives leached from the hemp shiv which are incorporated into the silica matrix inducing the binding effect. The composites were water resistant and showed good mechanical performance having the potential to develop novel thermal insulation building materials.

Keywords

Hemp; B. Adhesion; D. Chemical analysis; Mechanical testing

1. Introduction

Bio-based materials have become increasingly popular for producing economical engineering materials in the building and construction industry. Composites manufactured using the woody core of the hemp plant (*Cannabis Sativa* L.) known as shiv have been adopted by the building industry. Lightweight composites from hemp shiv possess excellent hygroscopic [1,2], thermal [3,4] and biodegradable [5] properties.

Hemp shiv has low density due to its high porosity and it tends to absorb large amounts of water [6]. The hydrophilic nature of bio-based materials makes them incompatible with hydrophobic thermoset/thermoplastic polymers [7]. On the other hand, since the shiv competes with the binder for the available water, purely hydraulic binders like lime or cement cannot hydrate completely, leading to a powdery inner core in the hemp-lime walls which is poorly bound [8]. The issue of adhesion with hemp-lime has stimulated considerable investment in hemp-specific lime based binders. The most recent generation of binders utilises high specific surface area lime in order to obtain a more reactive binder, however, they are still susceptible to adhesion issues. Pre-fabrication of panels or blocks ensures factory controlled conditions which reduce the extremes of adhesion issues (e.g. extensive flouring), but there still remains the inherent issue that the soluble sugars on the surface of the shiv interfere with the hydration of the binders, resulting in lower strength composites [9]. The durability of the material is compromised due to high moisture uptake as colonial fungal growth is encouraged resulting in cell wall degradation [10].

The major constituents of industrial hemp shiv are: cellulose (44%), hemicellulose (18-27%), lignin (22-28%) and other components such as extractives (1-6%) and ash (1-2%) [11,12]. Extractives include numerous low molecular mass compounds such as fatty acids, waxes, sterols, triglycerides, steryl esters, glycosides, fatty alcohols, terpenes, phenolics, simple sugars, alkaloids, pectins, gums and essential oils. It is well known that extractives can be isolated using polar and non-polar solvents. Volatile extractives are represented by highly volatile compounds which can be separated by water distillation. They are mainly composed of monoterpenes and other volatile terpenes including terpenoids as well as many different low

58 molecular weight compounds. Water-soluble compounds consist of various phenol compounds,

59 carbohydrates, glycosides and soluble salts, which can be extracted by cold or hot water [13–

60 15]. Lipophilic extractives are insoluble in water but soluble in organic solvents such as hexane,

61 dichloromethane, diethyl ether, acetone or ethanol [16]. Lipophilic extractives also known as

62 plant-resins are divided into free acids, e.g. resin acid and fatty acid, and neutral compounds,

63 e.g. fats and waxes. Extractives from bio-based materials can have a tacky nature forming pitch

64 deposits which is considered to be a major problem in the paper and pulp industry [17].

65

66 Natural fibre composites have low durability and tend to absorb large amounts of moisture

67 weakening interfacial adhesion and degradation, although this property can be improved by

68 treatment of the fibres [18–20]. Physical approaches such as plasma, ultraviolet or corona

69 treatment modify the fibre surface for enhancing roughness and interfacial adhesion. Chemical

70 treatments such as alkaline, silane and acetylation offer better improvements than physical

71 methods enhancing hydrophobicity and roughness of the fibres resulting in better interfacial

72 bonding [20–24]. Addition of silica particles into polymeric matrix has also been used to

73 enhance the mechanical properties of natural fibre reinforced composites [25]. Hydrolysed

74 silanes can chemically attach to the hydroxyl group of fibres, but they are known to provide only

75 a limited improvement in the mechanical properties of the resulting fibre composite due to their

76 physical compatibility with the matrix. The strength of natural fibre composites can be increased

77 if covalent bonds are present between the silane treated fibre and matrix [19,20]. Therefore

78 there is a need to develop novel composites that possess good interfacial bonding and at the

79 same time utilise the benefits of chemically treated bio-based aggregates being resistant to

80 water and degradation.

81

82 The work reported in this paper is carried out under the ISOBIO project which aims to develop

83 hygrothermally efficient bio-based building insulation panels with low embodied energy and low

84 embodied carbon. We have previously reported that the silica based treatment can provide

85 hydrophobicity to hemp shiv [26] without compromising its moisture buffering capacity as the

86 pores are not totally blocked by the coating [27]. The aim of this paper is to demonstrate the use

87 of a hydrophobic silica treatment as a binder for hemp shiv to produce novel robust light weight

88 composites with enhanced water resistance.

89

90 **2. Materials**

91 Hemp shiv used in this study was received from CAVAC, an agricultural cooperative based in

92 north-west France. Tetraethyl orthosilicate (TEOS, 98%), hexadecyltrimethoxysilane (HDTMS,

93 85%), nitric acid (70%) and absolute ethanol were obtained from Sigma-Aldrich.

94

95 **2.1 Silica formulation and preparation**

96 The silica based binder was synthesised by hydrolysis and condensation of TEOS in ethanol

97 and water. The reaction was catalysed by nitric acid. For the preparation of the silica, 1M of

98 TEOS was added to a mixture of 4M distilled water, 4M of absolute ethanol and 0.005M of nitric

99 acid. 0.015M of HDTMS was added to the above mixture as the hydrophobic agent. The sol

100 was vigorously stirred at 40 °C and atmospheric pressure for nearly 2 hours. The sols were

101 allowed to age for 96 hours in closed container at room temperature.

102

103 For the preparation of the silica glass, the sol was aged in a container at room temperature until

104 the gel point was reached. The gel-point was taken as the time when the sol did not show any

105 movement on turning the container upside down. For analysis of the binder, the left-over sol

106 contaminated with leached out hemp shiv extractives was aged in a container until the gel point

107 was reached and the specimen was termed the "binding matrix". A schematic illustration of silica

108 glass has been presented in Figure 1.

109

4
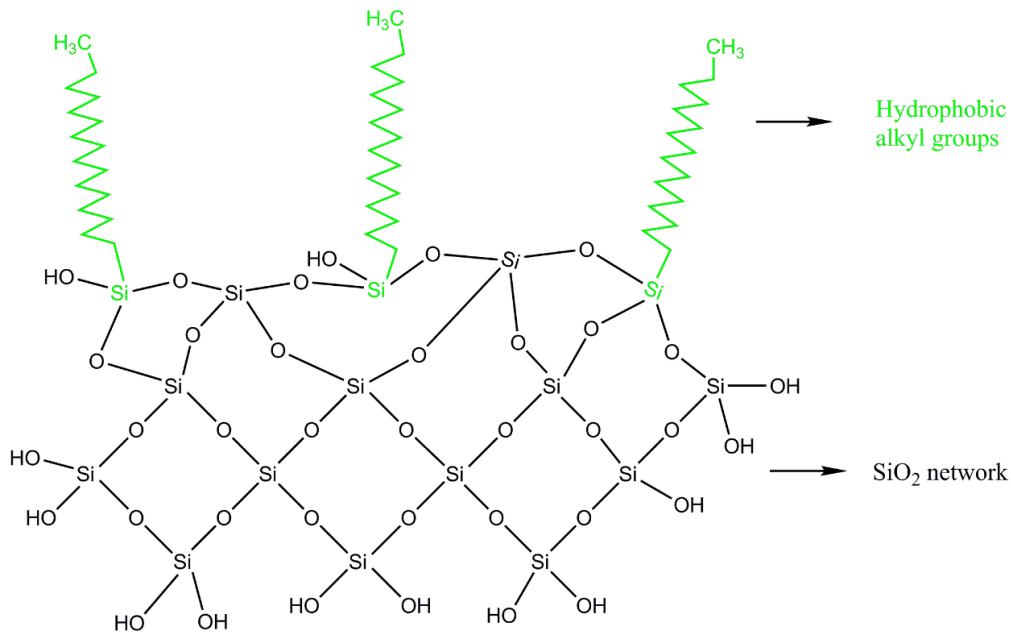
Figure 1. Schematic illustration of the silica glass.

2.2 Binder characterisation

The surface morphology of the specimens was characterised using a scanning electron

microscope (SEM), JEOL Corporation Model SEM-6480LV (Tokyo, Japan) operating at an

accelerating voltage of 10 kV. The specimens were coated with gold using an HHV500 sputter

coater (Crawley, UK) to prevent charging and to achieve high quality images of morphological

characteristics. Energy dispersive X-ray spectroscopy (Oxford INCA) was used to characterise

the elemental composition of the specimens.

The surface elemental and chemical composition of the specimens were analysed using X-ray

photoelectron spectroscopy (XPS). Prior to XPS analysis, samples were oven-dried at 80 °C for

96 hours. XPS spectra of the samples were recorded with an X-ray photoelectron spectrometer

(Kratos Axis Ultra, UK). All spectra were collected using a monochromatic Al Kα X-ray source

operated at 300 watts. The lateral dimensions of the samples were 800 microns × 400 microns,

corresponding to spot size of the Al Kα X-ray used, and probing depth was approximately 5

nanometres. For each sample, two spectra were recorded: (i) survey spectra (0–1150 eV, pass

energy 160 eV, and step size 1eV) recorded for apparent composition calculation; and (ii) high-

resolution C1s, O1s and Si 2p spectra (within 20 eV, pass energy 20 eV and step size within

130 0.05eV) recorded to obtain information on chemical bonds. Calculation of the apparent relative

131 atomic concentrations was performed with the CasaXPS software. Peak fitting was performed

132 with CasaXPS, which automatically and iteratively minimizes the difference between the

133 experimental spectrum and the calculated envelope by varying the parameters supplied in a first

134 guess.

135

136 Thermal analysis of the samples was carried out by simultaneous thermogravimetric analysis

137 (TGA) and differential scanning calorimetry (DSC) using the STA 449 F1 Jupiter thermal

138 analyser (Netzsch, Germany). The specimens were heated at a rate of 10 °C/min from 25 to

139 950 °C under nitrogen atmosphere purged at 30 ml/min using an alumina crucible.

140

141 **2.3 Extractive Analysis**

142 For isolation of the extractives, oven dried hemp shiv pieces were immersed in a solution

143 containing a mixture of ethanol and water in the molar ratio 1:1 to represent the solvent ratio

144 used in the sol formulation. Extraction of the hemp shiv samples was done using Soxhlet

145 apparatus for 2 h at 80 °C. The extract was evaporated to dryness using a rotary evaporator

146 and placed overnight in a vacuum oven. The dried extract was re-suspended in hexane and

147 methylene chloride for chromatographic analysis of the lipophilic fraction. Gas chromatography–

148 mass spectrometry (GC-MS) analysis was performed on a Varian CP 3800 gas chromatograph

149 coupled to a mass spectrometer detector (Varian Saturn 2000 MS/MS, 40-650 a.m.u.). The GC

150 oven was kept at 50 °C for 5 min and then heated to 250 °C at 5 °C/min. The final temperature

151 was held for 2 min. The injector temperature was set at 250 °C. Helium was used as the carrier

152 gas at a flow rate 1.0 ml/min. 1 µl of oil (solvent extractive) was injected using a rear injector

153 type 1177 with a split ratio 1:10. The spectrometer was operated in the electron impact mode

154 using 30 µA emission current and mass range m/z 40-600. Peaks were quantified by area and

155 the compounds were identified by comparing the mass spectra with those from Wiley and NIST

156 computer libraries.

157

158 **2.4 Preparation of composite samples**

159 Mixing of the constituent materials, hemp shiv (75 vol%) and sol (25 vol%), were carried out

160 manually to achieve a uniform mixture. The mass of the materials was pre-calculated to target a

161 final density of 175 kg/m^3 for the composites. Aggregates of hemp shiv were mixed with the sol

162 and then placed into a phenolic ply mould, tamped down and left overnight in the oven at 80 °C.

163 The specimens were removed from the moulds and transferred to a conditioning room at 19 °C

164 and 50% relative humidity. Another set of samples were prepared by mixing hemp shiv (75

165 vol%) and ethanol-water solution (25 vol%) and rest of the conditions were kept constant as

166 described above.

167

168 **2.5 Composite characterisation**

169 Compressive tests were conducted on 100mm cube samples using an Instron 50 KN testing rig

170 at a controlled displacement rate of 3 mm/min; the inbuilt instrumentation was used to both

171 record load and platen displacement at a resolution of one data point per 0.1 s. A durability test

172 was performed to determine the robustness of the binder. Composite samples were fully

173 immersed in water for 24 hours at 20 °C. The samples were removed from water and placed in

174 an oven at 80 ° for complete drying until no further mass change was observed. Compression

175 tests were performed on these samples and the results were compared with control samples.

176 Prior to compression testing, the samples were placed in a conditioning room at 19 °C and 50%

177 relative humidity for at least 24 hours. The tests were performed in triplicate and the average

178 reading was reported.

179

180

181

182

183

184

185

186　**3. Results**

187　**3.1 Morphology characterisation**

188　The morphology of the silica glass, hemp shiv composite and the binding matrix is presented in

189　Figure 2. The silica glass (figure 2A) has a smooth texture and is classically brittle when

190　compared to the binding matrix (Figure 2B) which exhibits some spallation. In general, the hemp

191　shiv particles are well embedded in the matrix due good interaction between the hemp shiv and

192　binding matrix. However, some minor cracks appear in the matrix (Figure 2C) which could be a

193　result of shrinkage during drying of the gel.

194

195

196
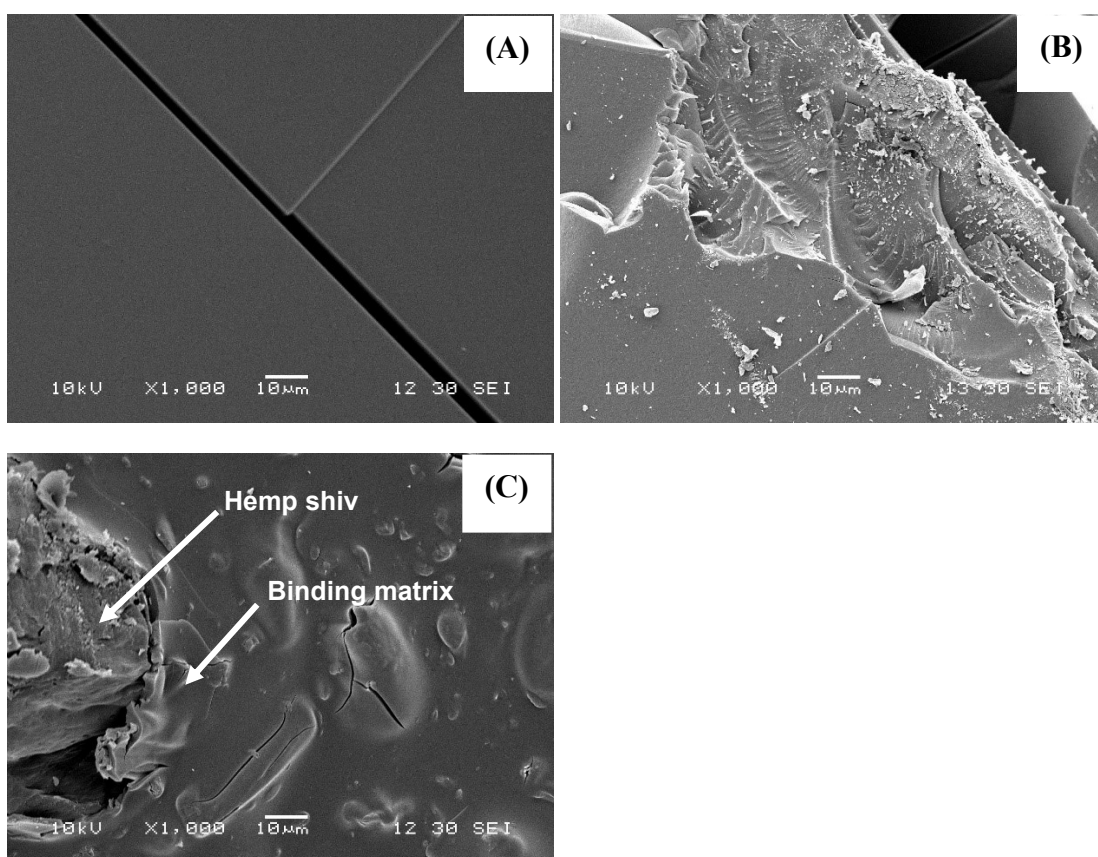
197　Figure 2. SEM micrographs of (A) silica glass, (B) binding matrix and (C) hemp shiv composite.

198

199　**3.2 Chemical characterisation**

200　The EDX analysis (Table 1) shows the surface composition of the silica specimens. The

201　percentage of carbon is significantly higher in the binding matrix than the silica glass. The

202　presence of carbon in the silica glass is due to the alkyl groups providing functionalisation.

203

204   Table 1. EDX analysis of silica glass and binding matrix.

Element	Silica glass		Binding matrix	
	Weight %	Atomic %	Weight %	Atomic %
C K	19.41 ± 3.8	28.69 ± 4.5	51.45 ± 5.3	61.94 ± 4.9
O K	43.21 ± 3.3	51.07 ± 7.1	34.86 ± 3.2	31.65 ± 3.7
Si K	43.33 ± 7.6	29.48 ± 7.3	7.15 ± 1.8	3.71 ± 1.1
Other	0.35 ± 0.1	0.26 ± 0.1	6.54 ± 0.2	2.69 ± 0.2

205

206   The chemical composition of the silica glass and the binding matrix was determined by X-ray

207   photoelectron spectroscopy. The atomic percentage of various elements present at the sample

208   surface was determined by a low-resolution survey scan. The relative elemental composition for

209   the specimens is listed in Table 2.

210

211   Table 2. Relative amount of atoms in the sample determined by low-resolution XPS scan.

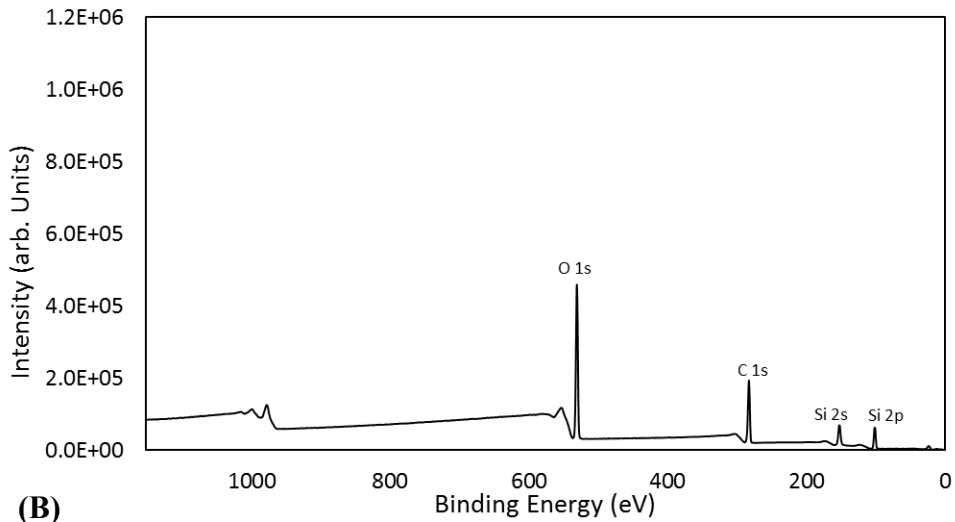| Element	Relative Concentration (Atomic %)	
	Silica Glass	Binding matrix
C	19.86	46.09
O	61.50	40.34
Si	18.64	13.58

212

213   The main elements detected for both the silica specimens were carbon, oxygen and silicon. The

214   binding matrix showed higher content of carbon as seen in Figure 3.

215
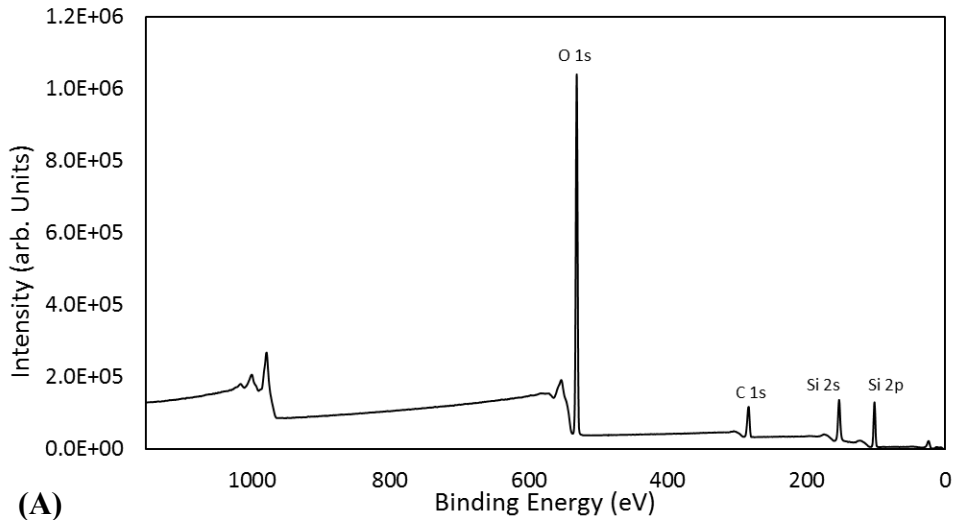
216 **(A)**

217 **(B)**

218 Figure 3. XPS survey scan for (A) silica glass, (B) binding matrix.

219

220 A high-resolution scan was performed on the C1s region for the silica glass and the binding

221 matrix (Figure 4) to determine the type of oxygen-carbon bonds present. The chemical bond

222 analysis of carbon was performed by curve-fitting the C1s peak and deconvoluting it into four

223 sub peaks corresponding to unoxidized carbon C1, and various oxidized carbons C2, C3 and

224 C4. The binding energy, corresponding bond type and their relative percentage are listed in

225 Table 3. The silica based binder shows additional oxidised carbon sub peaks, C3 and C4.

226

227   Table 1. Deconvoluted peak parameters and relative amount of different carbon-to-oxygen

228   bonds at sample surface determined by high-resolution XPS.

| Carbon Group	Peak parameters		Relative amount (% area)	
	Binding Energy (eV)	Bond	Silica Glass	Binding matrix
C1	285.0	C-C or C-H	68.65	84.30
C2	286.6/286.8	C-OH	31.35	10.40
C3	288.0	O-C-O or C=O	0.00	4.50
C4	289.2	O-C=O	0.00	0.81

229

230   The C1s high resolution spectra with the deconvoluted peaks for silica glass and binding matrix

231   are represented in Figure 4. The C1 peak is related carbon-carbon or carbon-hydrogen bonds

232   whereas C2, C3, and C4 peaks are associated with carbon-oxygen bonds.
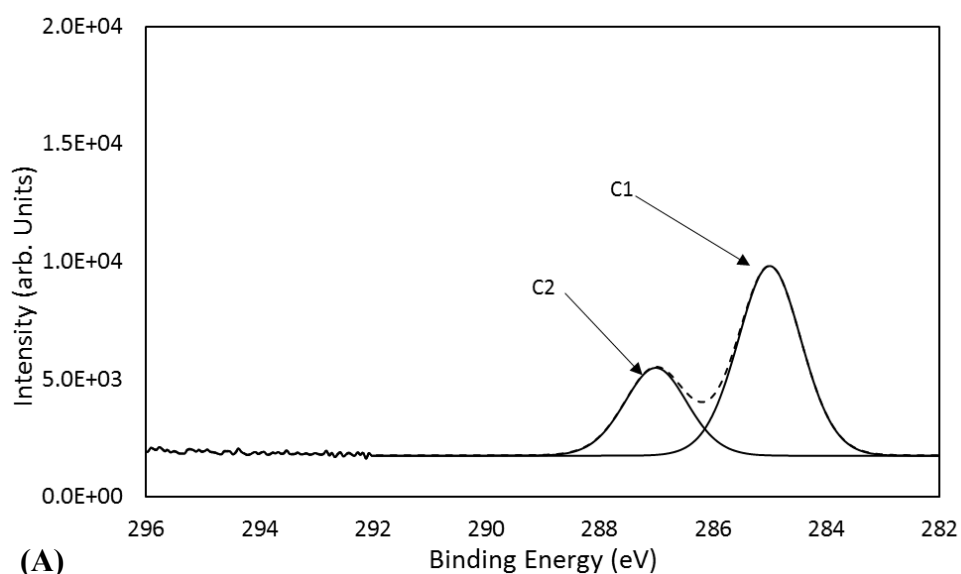
233   **(A)**
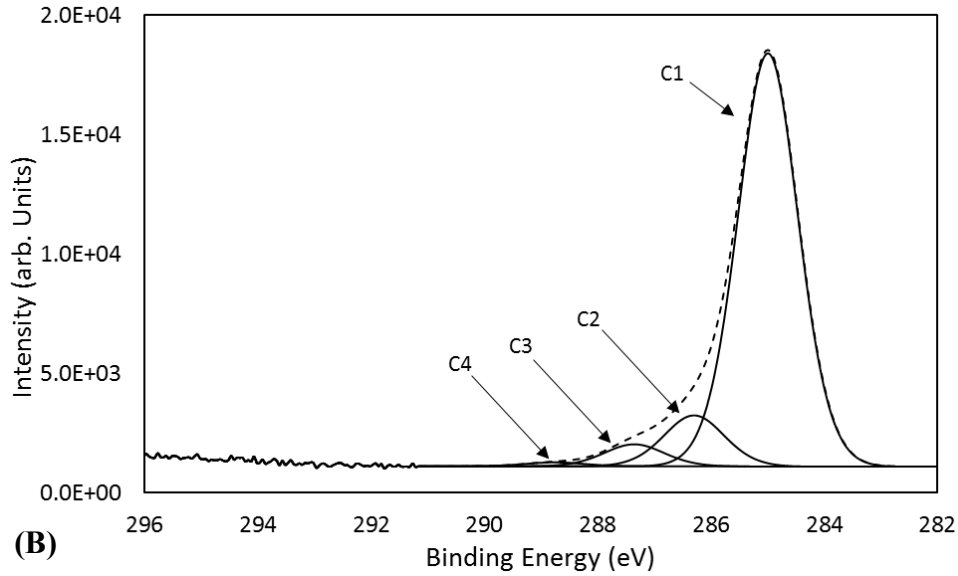
Figure 4. XPS scan of C1s region for (A) silica glass, (B) binding matrix.

3.3 Physical characterisation

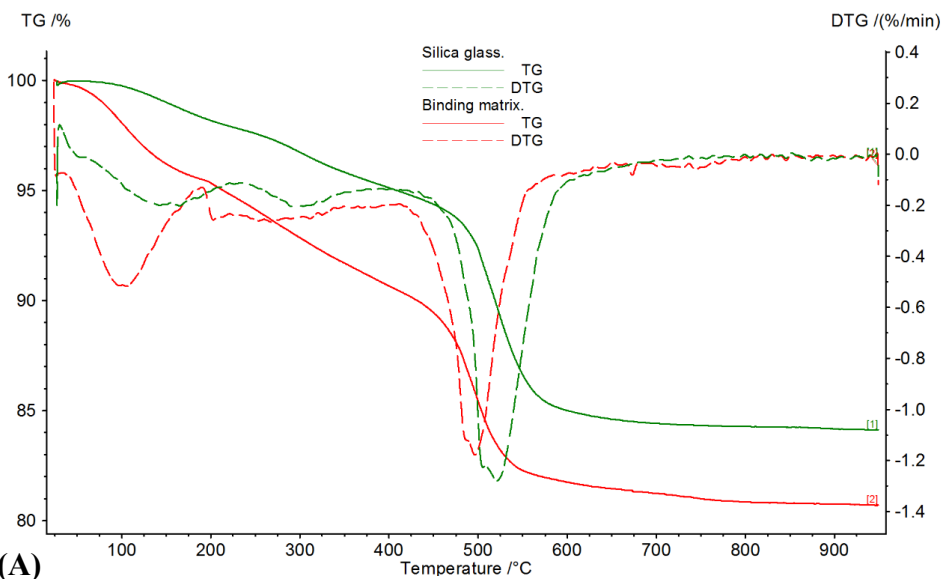The thermal analysis of the silica glass and the binding matrix is reported in Figure 5. From the TGA weight loss curves, it is seen that silica glass has a residual mass of 84.1% whereas the binding matrix has a resi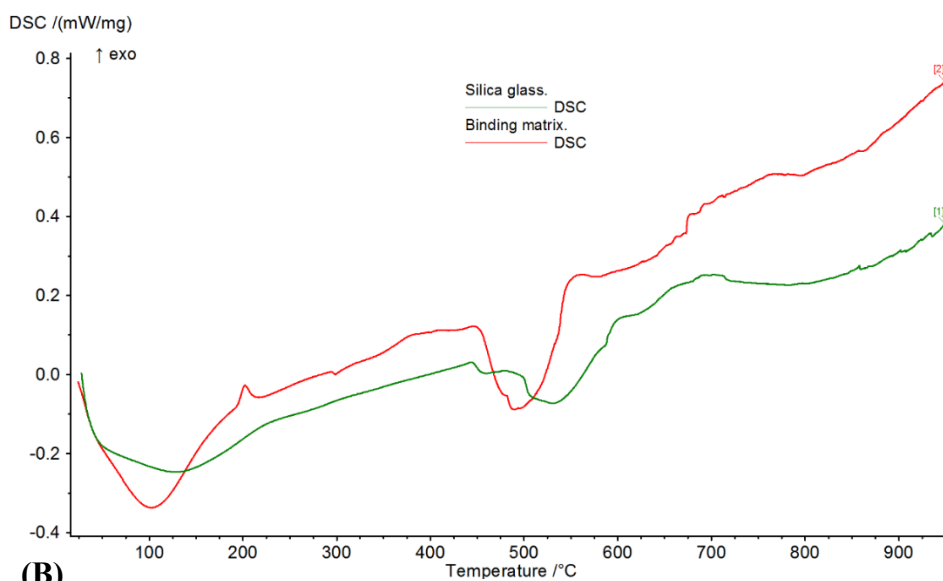dual mass of 80.7% at 950 °C. The maximum decomposition peak determined from the first derivative of the weight loss thermogram (DTG) curve is at 525 °C for silica glass and 495 °C for the binding matrix.

(B)

Figure 5. Thermal analysis of silica glass and binding matrix; (A) TGA and DTG curves, (B) DSC curves.

The DSC graph of the binding matrix shows a stronger endothermic peak at 102 °C when compared to the endothermic peak at 128 °C for silica glass. The endothermic peaks corresponding to the maximum decomposition rate are at 489 °C and 530 °C for the binding matrix and silica glass respectively.

3.4 Identification of Extractives

The identification of the extracted compounds was performed using GCMS. The polar components of the extractives were analysed for identification of the lipophilic extractives which are responsible for their tacky nature [28] and would contribute to the adhesive properties of the binding matrix. The yield of total extractives (polar and non-polar) in hemp shiv was 6.23% (dry weight %). The hexane yield and methylene chloride yield in the total extract was 9.05% and 5.00% respectively.

The chromatographs for hexane extract and methylene chloride extract are presented in Figures 6 and 7 respectively. All the compounds identified by GCMS are listed in Tables 4 and 5. The individual compounds were identified based on a comparison with GC retention times and mass spectra from the NIST library. Over twenty compounds were identified in the hexane

265 extract and twelve compounds were identified in the methylene chloride extract. For the

266 analysis of the GCMS data, peaks lower than 30000 counts were rejected. From the

267 chromatograms, it was determined that fatty acids esters, mainly lauric acid and phthalic acid,

268 gave the highest peaks.
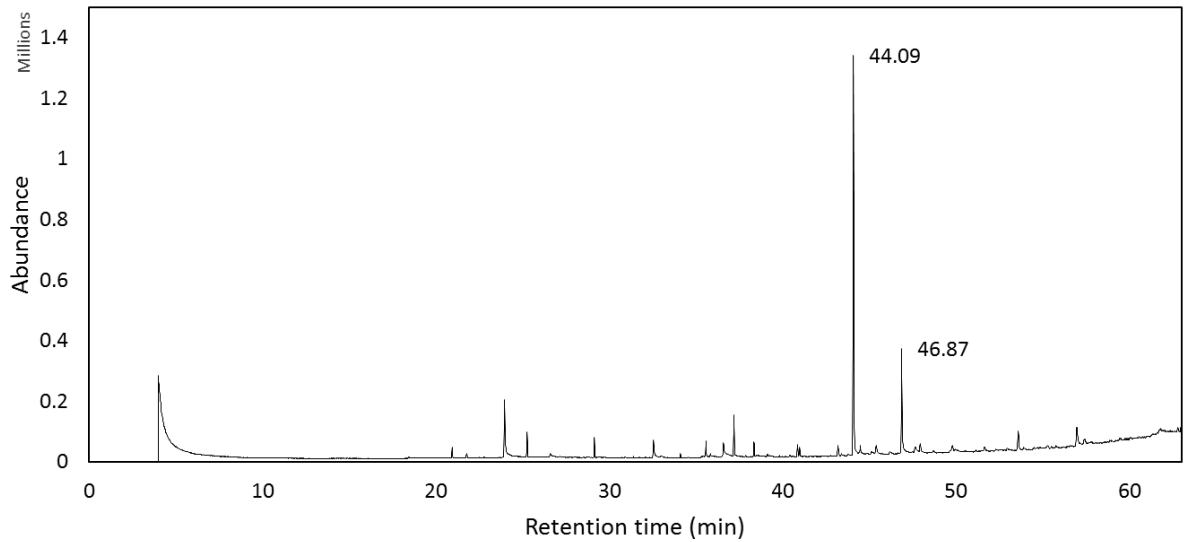
269

270 Figure 6. The chromatogram of hexane extractives from hemp shiv.

271
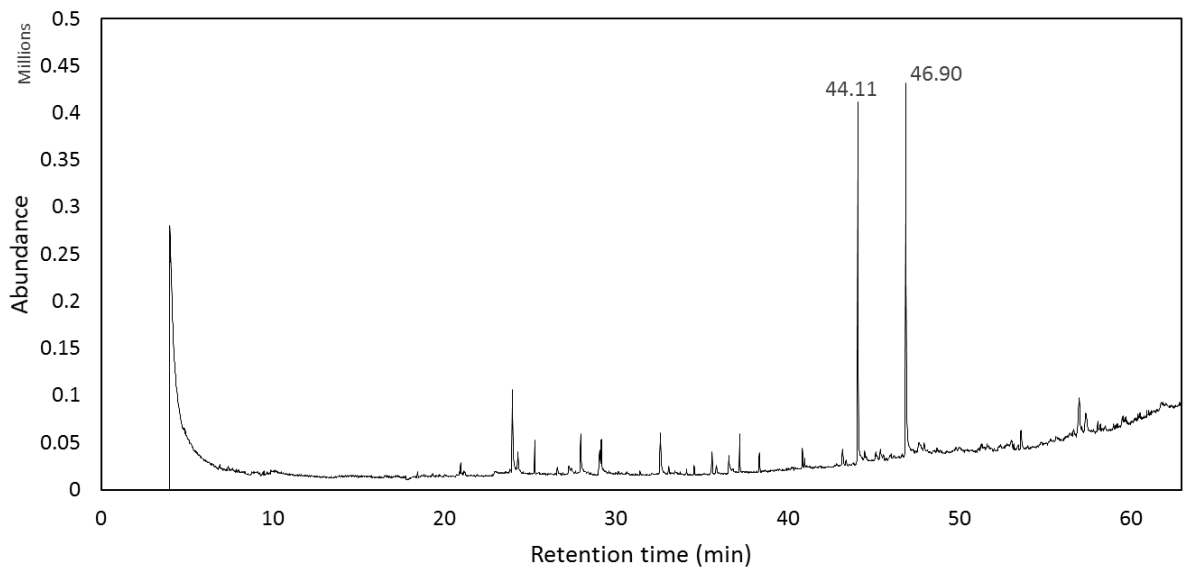
272

273 Figure 7. The chromatogram of methylene chloride extractives from hemp shiv.

274

275

14

276   Table 4. GCMS peak area and retention time of lipophilic extractives identified in hemp shiv

277   hexane extract.

Compound (Hexane Extract)	Retention time (min)	Peak Area
4-Hydroxy-3-nitrobenzaldehyde	23.961	732645
14-Methyl-8-hexadecen-1-ol	34.108	42090
Pentadecanoic acid	36.601	235957
Hexadecanoic acid, ethyl ester	37.202	346033
Heptadecanoic acid, 15-methyl-, ethyl ester	40.988	79364
Tetradecanal (Myristaldehyde)	43.402	32795
Dodecanoic acid (lauric acid), tetradecyl ester	44.086	4120000
Heptadecanoic acid, ethyl ester	44.484	94511
Oleyl alcohol	45.124	37702
1,2-Benzenedicarboxylic acid (phthalic acid), isodecyl octyl ester	46.872	1124000
Tricosanoic acid, methyl ester	47.939	159469
13-Heptadecyn-1-ol	48.691	31836
Tetracosanoic acid, methyl ester	49.676	33092
Eicosanoic acid	49.815	181870
Hexadecanoic acid, octadecyl ester	51.163	31625
Pentacosanoic acid, methyl ester	51.658	113374
Ergost-5-en-3-ol	52.97	48769
Tricosane	53.592	327306
9,19-Cyclochloestene-3,7-diol,4,14-dimethyl-,3-acetate	53.91	38821
Cholestra-4,6 dien-3-ol	55.287	88534
Stigmasterol	55.784	34398
7-Dehydrodiosgenin	56.974	371899
Stigmastan-3-ol, 5-chloro-, acetate, (3.beta.,5.alpha.)	57.416	91981
Stigmastan-3-ol, 5-chloro-, acetate, (3.beta.,5.alpha.)	57.447	81052

278

279

280 Table 5. GCMS peak area and retention time of lipophilic extractives identified in methylene

281 chloride extract of hemp shiv.

| Compound (Methylene Chloride Extract)	Retention time (min)	Peak Area
4-Hydroxy-3-nitrobenzaldehyde	23.97	450485
2,6-Dimethoxybenzoquinone	27.945	287931
4-Hydroxy-3-nitrobenzoic acid	29.049	93543
Phenol,2,4-dinitro-6-methoxy	32.602	216393
Pentadecanoic acid	36.589	65679
Hexadecanoic acid, ethyl ester	37.221	111908
Octadecanoic acid, ethyl ester	41.011	28187
Dodecanoic acid (lauric acid), tetradecyl ester	44.108	1.70E+06
1,2-Benzenedicarboxylic acid (phthalic acid), mono(2-ethylhexyl) ester	46.899	2.75E+06
Octadecane, 3-ethyl-5-(2-ethylbutyl)-	53.625	106470
Stigmasta-5, 22-dien-3-ol, acetate, (3.beta.)-	57.009	348774
Cholest-1-eno[2,1-a]naphthalene,3',4'-dihydro-	57.396	263327

282

283 **3.5 Composite characterisation**

284 The compression testing of the composite samples prepared with hemp shiv and binding matrix

285 is imaged in Figure 8 and stress versus strain curves for the before and after immersion

286 samples are presented in Figure 9. The moisture sensitivity of the composite was determined by

287 comparing the mechanical properties of the hemp shiv composite before and after immersion in

288 water for 24 hours. Preparation of composite samples using hemp shiv and ethanol-water

289 solution (see section 2.4) was unsuccessful as the hemp shiv particles were not able to bind.

290

291 From Figure 9, the results from three test samples before immersion reveal that the composite

292 reaches an average compressive stress of 0.48 ± 0.02 MPa at 30% strain. After the immersion

293 test, a slight reduction in compressive stress by 15% was observed for the three samples and

294 the average reading was 0.41 ± 0.01 MPa at 30% strain. It was noted that further compression

295 led to densification of the sample. After compression, the sample showed some elastic

296 behaviour as seen in Figure 8.

297

298
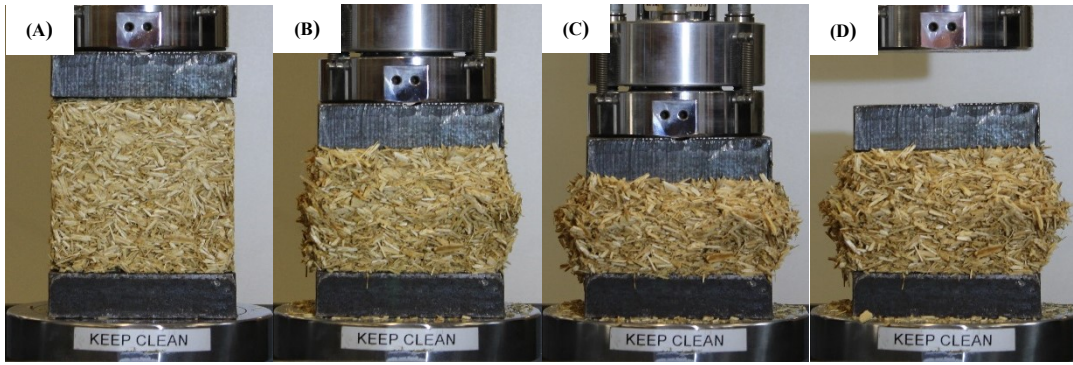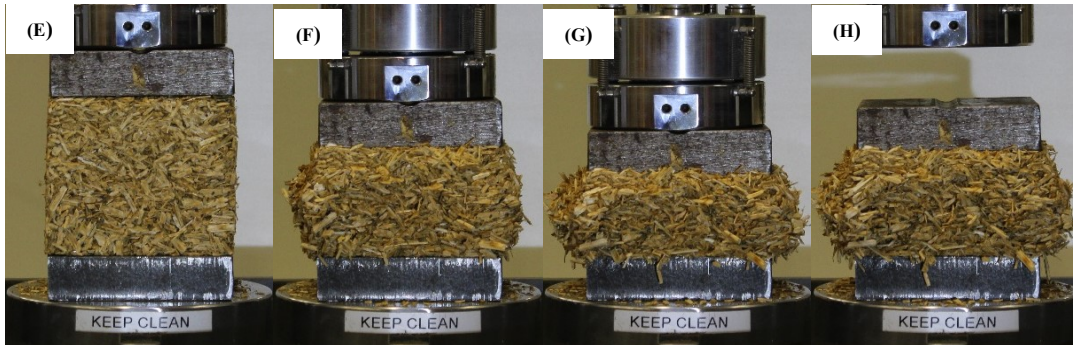
Figure 8. Compression testing of hemp shiv composites at; (A) 0% strain, (B) 30% strain, (C) 50% strain, (D) after 50% strain, and after immersion in water at (E) 0% strain, (F) 30% strain, (G) 50% strain, (H) after 50% strain.

302

303

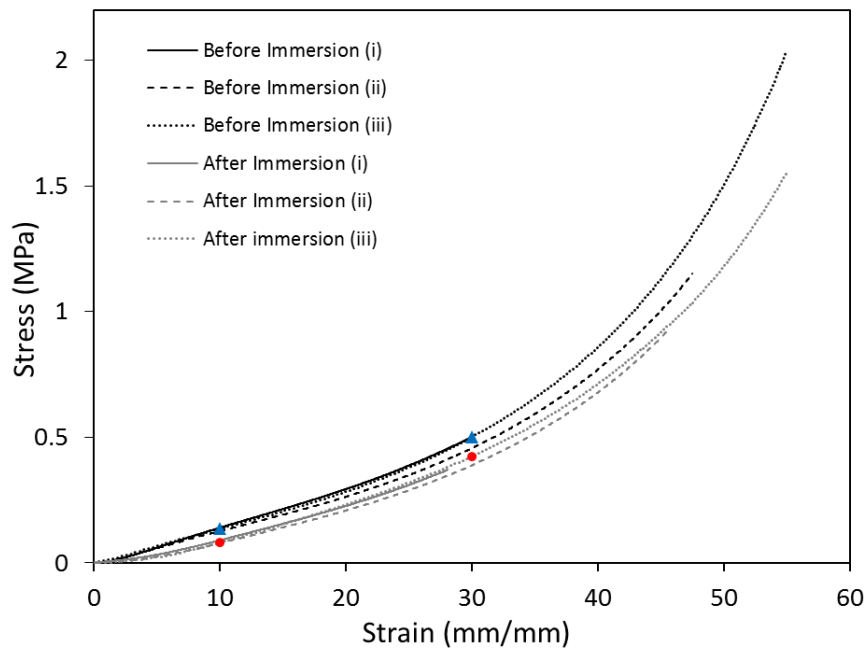**Figure 9. Compressive stress versus strain characteristics of hemp shiv composites before and after immersion in water.**

4. Discussion

In the present study, hemp shiv based composites have been manufactured by using silica sol as a binder. The binding matrix has been characterised and its morphology, chemical composition and physical properties have been studied in comparison with silica glass. The binder is prepared by the hydrolysis and condensation of TEOS in water in the presence of ethanol as the mediator solvent. HDTMS is added for functionalisation thereby providing hydrophobic alkyl groups in the silica network. The formulation has been used earlier for treatment of hemp shiv particles for imparting hydrophobicity to the material [26]. Here we report the binding properties of silica when mixed with hemp shiv. The silica sol interacts with hemp shiv leaching out extractives and waxes which leads to visual changes turning the silica matrix from colourless transparent to yellowish opaque.

The silica is able to covalently bond to hemp shiv through the hydroxyl groups of cellulose [26]. During the drying process, the gel starts condensing, releasing ethanol and water and develops a silica network. The extracts from the shiv that are entrapped in the silica network alter the characteristics of the silica. From the SEM analysis, it was seen that the silica morphology is modified. The structure of the new modified silica with incorporated extracts is less brittle when compared to the pure silica glass.

The chemical composition of the silica specimens is mainly composed of carbon, oxygen and silicon. Chemical characterisation using EDX reveals that the modified silica (binding matrix) has a higher carbon content than the pure silica. Detailed XPS analysis indicates that due to sol interaction with hemp shiv, the silica chemistry has been significantly altered. The surface carbon content of the binding matrix increased by 27% (from 19% to 46%). On the other hand, the oxygen content decreased by 21% (from 61% to 40%). This change in C/O ratio and increase in the surface carbon content can be attributed to the additional extracts that have been identified in the modified network of the binding matrix. The decrease in surface oxygen content can be related to the masking effect of the hemp shiv extracts reducing the detectability of the oxygen bonds in the silica network.

18

336   The C1s high resolution XPS spectra reveal that the hemp shiv extracts have modified the silica

337   network leading to the appearance of C3 and C4 peaks which are not present in the pure silica

338   glass. Furthermore, the increase in the intensity of the C1 component for the binding matrix

339   from 68% to 84% indicates the presence of C-C and C-H bonds from the incorporated extracts.

340   To analyse the extracts that were leaching out from hemp shiv during the silica based

341   treatment, the process was simplified by using a solution of ethanol and water for the extraction

342   process. Ethanol is able to dissolve waxes and isolate lipophilic extractives. These ethanol-

343   soluble extractives were analysed using GCMS and it was found that the extract was mainly

344   composed of lauric acid and phthalic acid with many other fatty acids. The majority of the

345   compounds identified using GCMS belong to the group of lipophilic extractives which are

346   hydrophobic in nature [16,29]. This could possibly be one of the factors for the compatibility

347   between the lipophilic extractives and the sol-gel chemistry due to their hydrophobic nature.

348

349   The thermal decomposition patterns of the silica specimens were studied by TGA. The binding

350   matrix had a higher weight loss below 100 °C and a greater endothermic peak that can be

351   attributed to the presence of fatty acids in addition to the physically adsorbed water [30]. The

352   embedded extracts in the silica network changed the decomposition range of the organic

353   fragments of the silane corresponding to the temperature range of 270-600 °C [31]. Due to the

354   higher percentage of the organic compounds in the binding matrix, the weight loss was greater

355   and a peak shift was observed in the first derivative of the weight loss thermogram (DTG). The

356   maximum decomposition rate in the DTG curve for silica glass was at 520 °C attributed to the

357   loss of silanol groups. The modification of silica network with hemp shiv extracts lowered the

358   thermal stability of the binding matrix.

359

360   Composites were prepared using hemp shiv and silica sol and their mechanical performance

361   was evaluated. The composites were light weight with a density of 175 kg/m^3 and the

362   compressive stress of 0.48 MPa attained at 30% strain is relatively good when compared to

363   other hemp shiv based composites such as hemp-lime (0.02 - 0.39 MPa at density 360 kg/m^3)

364   [32], hemp-starch (0.4 MPa at density 177 kg/m^3) [33] and hemp-clay (0.39 at density 373

365   kg/m^3) [34]. Higher strains corresponded with higher compressive stresses leading to

366 densification of the sample without reaching a failure point. This suggests that the interfacial

367 adhesion between the shiv and binding matrix is good and the shear forces are low.

368

369 After the immersion test, the decrease in mechanical strength can be related to the swelling of

370 the shiv when placed in water for 24 hours. Since the binder also provides hydrophobicity to the

371 hemp shiv, the compressive stress versus strain characteristics are not compromised to a great

372 extent. However, the swelling could be related to the slow penetration of water through micro-

373 cracks on the coated surface or due to the presence of small uncovered pores within the hemp

374 shiv. The binder can provide hydrophobicity to the hemp shiv but it cannot fully protect the hemp

375 shiv against long-term water interaction. The slight decrease in compressive stress reached at

376 30% strain can be attributed to the weakening of the interfacial bonding between the hemp shiv

377 and the binding matrix. However, composites produced using an ethanol-water mixture instead

378 of silica sol was unsuccessful as the hemp shiv fell apart on demoulding. The ethanol is

379 responsible for isolation of the extractives and waxes from hemp shiv but the extractives cannot

380 bind hemp shiv on their own. The extractives modify the silica chemistry and the binding matrix

381 holds the hemp particles together resulting in the production of coherent composite blocks.

382

383 When compared to conventional hemp-lime composites, it is evident that the production costs of

384 the hemp-silica composites would be higher due to the hydrophobic treatment on hemp shiv.

385 However, this cost could be off-set by savings elsewhere, both in production ingredients

386 (reduction in water usage, lower drying times) as well as an extension in service life, potentially

387 reducing the whole life cost. Moreover, the commercial availability of sol-gel solution on an

388 industrial scale would significantly lower the cost of this novel composite. The preparation of

389 hemp-silica composite results in the reduction of 2L of mixing water per 1kg of hemp shiv when

390 compared to a conventional hemp-lime composite. The thermal performance of the new

391 composite is expected to be better due to their significantly lower density than hemp-lime.

392 Overall early indications are that the global warming potential of this composite would be

393 approximately 5% lower than that of a conventional composite. The life span is expected to

394 increase by 50% due the improved resistance to water that is responsible for degradation of the

395 composite.

5. Conclusions

In this work, the novel use of sol-gel treatment as a binding agent has been identified, providing multi-functionality from a single treatment using a simple, economical one-step process. Thorough investigation of the binder and its chemical interaction with hemp shiv has been performed. Lipophilic extractives from the shiv are integrated within the silica network, modifying chemical, morphological and physical characteristics of the glass material. The prepared composites show good mechanical performance as a non-load bearing material and has great potential as a thermal insulation material due to their low density as well as the high porosity of hemp shiv. Durability tests evaluated the robustness of the composite and the hydrophobic silica treatment was seen to enhance the water resistance of the material. This study is applicable to not only the hemp shiv material but also to any bio-based material which has cellulose and lipophilic extractives in its composition. This therefore transforms the current use of the sol-gel treatment as a surface modifier agent alone to dual functionality as a binder agent leading to economical and sustainable bio-based building materials.

Disclosure statement

The authors declare that they have no conflict of interest.

References

[1]   Tran Le AD, Maalouf C, Mai TH, Wurtz E, Collet F. Transient hygrothermal behaviour of

426   a hemp concrete building envelope. Energy Build 2010;42:1797–806.

427   doi:10.1016/j.enbuild.2010.05.016.

428   [2] Latif E, Lawrence M, Shea A, Walker P. Moisture buffer potential of experimental wall

429   assemblies incorporating formulated hemp-lime. Build Environ 2015;93:199–209.

430   doi:10.1016/j.buildenv.2015.07.011.

431   [3] Benfratello S, Capitano C, Peri G, Rizzo G, Scaccianoce G, Sorrentino G. Thermal and

432   structural properties of a hemp-lime biocomposite. Constr Build Mater 2013;48:745–54.

433   doi:10.1016/j.conbuildmat.2013.07.096.

434   [4] Shea A, Lawrence M, Walker P. Hygrothermal performance of an experimental hemp-

435   lime building. Constr Build Mater 2012;36:270–5.

436   doi:10.1016/j.conbuildmat.2012.04.123.

437   [5] Theis M, Grohe B. Biodegradable lightweight construction boards based on

438   tannin/hexamine bonded hemp shaves. Holz Als Roh - Und Werkst 2002;60:291–6.

439   doi:10.1007/s00107-002-0306-0.

440   [6] Jiang Y, Lawrence M, Ansell MP, Hussain A. Cell wall microstructure, pore size

441   distribution and absolute density of hemp shiv. R Soc Open Sci 2018;5:171945.

442   doi:10.1098/rsos.171945.

443   [7] Gassan J, Gutowski VS, Bledzki AK. About the surface characteristics of natural fibres.

444   Surf Eng 2000;283:132–9. doi:10.1002/1439-2054(20001101)283:1<132::AID-

445   MAME132>3.0.CO;2-B.

446   [8] Elfordy S, Lucas F, Tancret F, Scudeller Y, Goudet L. Mechanical and thermal properties

447   of lime and hemp concrete ("hempcrete") manufactured by a projection process. Constr

448   Build Mater 2008;22:2116–23. doi:10.1016/j.conbuildmat.2007.07.016.

449   [9] Ahmad MR, Bing C, Oderji SY, Mohsan M. Development of a new bio-composite for

450   building insulation and structural purpose using corn stalk and magnesium phosphate

451   cement; Physical, mechanical, thermal and hygric evaluation. Energy Build 2018.

452   doi:10.1016/j.enbuild.2018.06.007.

453 [10] Marceau S, Glé P, Guéguen-Minerbe M, Gourlay E, Moscardelli S, Nour I, et al.

454   Influence of accelerated aging on the properties of hemp concretes. Constr Build Mater

455   2017;139:524–30. doi:10.1016/j.conbuildmat.2016.11.129.

456   [11]   Kidalova L, Stevulova N, Terpakova E. Influence of water absorption on the selected

457   properties of hemp hurds composites. Pollack Period 2015.

458   doi:10.1556/Pollack.10.2015.1.12.

459   [12]   Gandolfi S, Ottolina G, Riva S, Fantoni GP, Patel I. Complete chemical analysis of

460   carmagnola hemp hurds and structural features of its components. BioResources

461   2013;8:2641–56. doi:10.15376/biores.8.2.2641-2656.

462   [13]   PETTERSEN RC. The Chemical Composition of Wood 1984:57–126. doi:10.1021/ba-

463   1984-0207.ch002.

464   [14]   Yang G, Jaakkola P. Wood chemistry and isolation of extractives from wood. Lit Study

465   BIOTULI Proj Univ Appl Sci 2011:10–22.

466   [15]   S. M, D. Santana ALB, A. C, S. L, Bieber L. Phenolic Extractives and Natural Resistance

467   of Wood. Biodegrad - Life Sci 2013. doi:10.5772/56358.

468   [16]   Sun RC, Tomkinson J. Comparative study of organic solvent-soluble and water-soluble

469   lipophilic extractives from wheat straw 2: Spectroscopic and thermal analysis. J Wood

470   Sci 2002;48:222–6. doi:10.1007/BF00771371.

471   [17]   Gutiérrez A, Del Río JC, Martínez MJ, Martínez AT. The biotechnological control of pitch

472   in paper pulp manufacturing. Trends Biotechnol 2001;19:340–8. doi:10.1016/S0167-

473   7799(01)01705-X.

474   [18]   Kabir MM, Wang H, Lau KT, Cardona F, Aravinthan T. Mechanical properties of

475   chemically-treated hemp fibre reinforced sandwich composites. Compos Part B Eng

476   2012;43:159–69. doi:10.1016/j.compositesb.2011.06.003.

477   [19]   Xie Y, Hill CAS, Xiao Z, Militz H, Mai C. Silane coupling agents used for natural

478   fiber/polymer composites: A review. Compos Part A Appl Sci Manuf 2010;41:806–19.

479   doi:10.1016/j.compositesa.2010.03.005.

480   [20]   Pickering KL, Efendy MGA, Le TM. A review of recent developments in natural fibre

481   composites and their mechanical performance. Compos Part A Appl Sci Manuf

482   2016;83:98–112. doi:10.1016/j.compositesa.2015.08.038.

483   [21]   Valadez-Gonzalez A, Cervantes-Uc JM, Olayo R, Herrera-Franco PJ. Effect of fiber

484   surface treatment on the fiber-matrix bond strength of natural fiber reinforced

485   composites. Compos Part B Eng 1999;30:309–20. doi:10.1016/S1359-8368(98)00054-7.

486   [22]   Sepe R, Bollino F, Boccarusso L, Caputo F. Influence of chemical treatments on

487   mechanical properties of hemp fiber reinforced composites. Compos Part B Eng

488   2018;133:210–7. doi:10.1016/J.COMPOSITESB.2017.09.030.

489   [23]   Sullins T, Pillay S, Komus A, Ning H. Hemp fiber reinforced polypropylene composites:

490   The effects of material treatments. Compos Part B Eng 2017;114:15–22.

491   doi:10.1016/j.compositesb.2017.02.001.

492   [24]   Kabir MM, Wang H, Lau KT, Cardona F. Chemical treatments on plant-based natural

493   fibre reinforced polymer composites: An overview. Compos Part B Eng 2012;43:2883–

494   92. doi:10.1016/j.compositesb.2012.04.053.

495   [25]   Da Silva LJ, Panzera TH, Velloso VR, Christoforo AL, Scarpa F. Hybrid polymeric

496   composites reinforced with sisal fibres and silica microparticles. Compos Part B Eng

497   2012;43:3436–44. doi:10.1016/j.compositesb.2012.01.026.

498   [26]   Hussain A, Calabria-Holley J, Schorr D, Jiang Y, Lawrence M, Blanchet P.

499   Hydrophobicity of hemp shiv treated with sol-gel coatings. Appl Surf Sci 2018;434:850–

500   60. doi:10.1016/j.apsusc.2017.10.210.

501   [27]   Hussain A, Calabria-Holley J, Jiang Y, Lawrence M. Modification of hemp shiv properties

502   using water-repellent sol–gel coatings. J Sol-Gel Sci Technol 2018. doi:10.1007/s10971-

503   018-4621-2.

504   [28]   Marques G, del Río JC, Gutiérrez A. Lipophilic extractives from several nonwoody

505   lignocellulosic crops (flax, hemp, sisal, abaca) and their fate during alkaline pulping and

506   TCF/ECF bleaching. Bioresour Technol 2010;101:260–7.

507   doi:10.1016/j.biortech.2009.08.036.

508   [29]   Hardell HL, Nilvebrant NO. A rapid method to discriminate between free and esterified

509   fatty acids by pyrolytic methylation using tetramethylammonium acetate or hydroxide. J

510   Anal Appl Pyrolysis 1999;52:1–14. doi:10.1016/S0165-2370(99)00035-2.

511   [30]   Knothe G, Dunn RO. A Comprehensive Evaluation of the Melting Points of Fatty Acids

512   and Esters Determined by Differential Scanning Calorimetry. J Am Oil Chem Soc

513   2009;86:843–56. doi:10.1007/s11746-009-1423-2.

514   [31]   Hemsri S, Asandei AD, Grieco K, Parnas RS. Biopolymer composites of wheat gluten

515   with silica and alumina. Compos Part A Appl Sci Manuf 2011;42:1764–73.

24

516   doi:10.1016/j.compositesa.2011.07.032.

517   [32]   Walker R, Pavia S, Mitchell R. Mechanical properties and durability of hemp-lime

518   concretes. Constr Build Mater 2014;61:340–8. doi:10.1016/j.conbuildmat.2014.02.065.

519   [33]   Benitha Sandrine U, Isabelle V, Ton Hoang M, Maalouf C. Influence of chemical

520   modification on hemp-starch concrete. Constr Build Mater 2015;81:208–15.

521   doi:10.1016/j.conbuildmat.2015.02.045.

522   [34]   Mazhoud B, Collet F, Pretot S, Lanos C. Mechanical properties of hemp-clay and hemp

523   stabilized clay composites. Constr Build Mater 2017;155:1126–37.

524   doi:10.1016/j.conbuildmat.2017.08.121.

525